Host-mediated impairment of parasite maturation during blood-stage *Plasmodium* infection

David S. Khoury[a], Deborah Cromer[a], Jasmin Akter[b], Ismail Sebina[b], Trish Elliott[b], Bryce S. Thomas[b], Megan S. F. Soon[b], Kylie R. James[b], Shannon E. Best[b], Ashraful Haque[b,1,2], and Miles P. Davenport[a,1,2]

[a]Infection Analytics Program, Kirby Institute, The University of New South Wales, Kensington, NSW 2052, Australia; and [b]Malaria Immunology Laboratory, QIMR Berghofer Medical Research Institute, Herston, Brisbane, QLD 4006, Australia

Edited by Andrew F. Read, The Pennsylvania State University, University Park, PA, and accepted by Editorial Board Member Diane E. Griffin June 7, 2017 (received for review November 17, 2016)

Severe malaria and associated high parasite burdens occur more frequently in humans lacking robust adaptive immunity to *Plasmodium falciparum*. Nevertheless, the host may partly control blood-stage parasite numbers while adaptive immunity is gradually established. Parasite control has typically been attributed to enhanced removal of parasites by the host, although in vivo quantification of this phenomenon remains challenging. We used a unique in vivo approach to determine the fate of a single cohort of semisynchronous, *Plasmodium berghei* ANKA- or *Plasmodium yoelii* 17XNL-parasitized red blood cells (pRBCs) after transfusion into naive or acutely infected mice. As previously shown, acutely infected mice, with ongoing splenic and systemic inflammatory responses, controlled parasite population growth more effectively than naive controls. Surprisingly, however, this was not associated with accelerated removal of pRBCs from circulation. Instead, transfused pRBCs remained in circulation longer in acutely infected mice. Flow cytometric assessment and mathematical modeling of intraerythrocytic parasite development revealed an unexpected and substantial slowing of parasite maturation in acutely infected mice, extending the life cycle from 24 h to 40 h. Importantly, impaired parasite maturation was the major contributor to control of parasite growth in acutely infected mice. Moreover, by performing the same experiments in *rag1*$^{-/-}$ mice, which lack T and B cells and mount weak inflammatory responses, we revealed that impaired parasite maturation is largely dependent upon the host response to infection. Thus, impairment of parasite maturation represents a host-mediated, immune system-dependent mechanism for limiting parasite population growth during the early stages of an acute blood-stage *Plasmodium* infection.

malaria | clearance | mathematical modelling | *Plasmodium berghei* ANKA | parasite maturation

Blood-stage *Plasmodium* infection involves sequential rounds of red blood cell (RBC) invasion, intracellular parasite maturation, asexual replication, RBC rupture, and release of invasive merozoite forms into the bloodstream. Depending on the species, each cycle of infection takes ∼24–72 h to complete, and between 8 and 32 merozoites are released from each rupturing parasitized RBC (pRBC). In a naive individual infected with *Plasmodium falciparum*, the total number of pRBCs in the bloodstream increases by around 10-fold each cycle [referred to here as a parasite multiplication factor (PMF) of 10] (1). The PMF can be reduced by a number of mechanisms, including antibody-mediated and adaptive T-cell–mediated immunity to the parasite. Naturally acquired adaptive immunity to malaria can take years to develop in endemic regions, with high parasite burdens and severe disease more common in those individuals yet to develop protective immunity, e.g., young children (2–4). Nevertheless, other aspects of the host response to infection, such as innate immune responses, may influence malaria parasite control (5), for example by inducing fever, enhancing phagocyte function, or contributing to the organ-specific pathology (6–8).

Blood-stage *Plasmodium* infections in mice have been used extensively to study innate and adaptive immune responses during malaria (7, 9–11). Use of these experimental models has revealed that during acute infection, specifically before an effective parasite-specific antibody response has developed, the host is able to partially control parasite growth (or in other words, to limit the PMF) (12–14). However, the precise mechanisms by which the PMF is reduced in vivo remain unclear. A number of potential innate control mechanisms have been suggested. In particular, the mechanical removal of pRBCs by the spleen (8, 15–18) [or liver (19)] is believed to be a primary mechanism by which the host controls the PMF (12). However, few studies have attempted to directly measure host removal of pRBCs in vivo (13, 19).

Here, we followed the fate of a single cohort of fluorescently labeled, semisynchronous *Plasmodium berghei* ANKA (*Pb*A) and *Plasmodium yoelii* 17XNL (*Py*) pRBCs when transfused into naive or acutely infected mice. Specifically, we compared the rate of removal of pRBCs from the bloodstream between these groups. Surprisingly, rather than observing an increase in pRBC removal due to a splenic and systemic inflammatory response, we observed increased parasite persistence in the circulation of acutely infected mice. Flow cytometric assessments and mathematical modeling showed that pRBCs persisted in circulation because they matured more slowly, taking longer than usual to complete their asexual life cycle. The phenomenon of impaired parasite maturation accounted for most of the improved control of infection in acutely infected mice and, furthermore, was largely driven by the host's response to infection.

Significance

Adaptive immunity to *Plasmodium falciparum* takes years to develop in endemic regions, leaving young children vulnerable to high parasite burdens and severe malaria. Host innate immune responses clearly occur during infection and may control parasite numbers in nonimmune individuals, for example by accelerating parasite removal from circulation. However, evidence of whether and how this occurs in vivo remains sparse. We set out to measure host removal of parasites during acute blood-stage *Plasmodium* infection in mice. However, rather than being removed more rapidly, parasites unexpectedly persisted in circulation. Persistence resulted from host-dependent slowing of parasite maturation. Thus *Plasmodium* maturation within red blood cells does not occur at a constant rate in vivo and can be influenced by the host itself.

Author contributions: D.S.K., D.C., A.H., and M.P.D. designed research; D.S.K., J.A., I.S., T.E., B.S.T., M.S.F.S., K.R.J., S.E.B., and A.H. performed research; D.S.K., D.C., and M.P.D. analyzed data; and D.S.K., D.C., A.H., and M.P.D. wrote the paper.

The authors declare no conflict of interest.

This article is a PNAS Direct Submission. A.F.R. is a guest editor invited by the Editorial Board.

[1]A.H. and M.P.D. contributed equally to this work.

[2]To whom correspondence may be addressed. Email: m.davenport@unsw.edu.au or Ashraful.Haque@qimrberghofer.edu.au.

This article contains supporting information online at www.pnas.org/lookup/suppl/doi:10.1073/pnas.1618939114/-/DCSupplemental.

Results

Donor Parasites Are Detected in Circulation for Longer in Acutely Infected Animals. Infection of C57BL/6J mice with *Pb*A elicits a rapid increase in parasitemia until day 4 postinfection (p.i.), followed by a slowing in the growth rate of parasites (14). To reveal factors causing this slowed growth, we sought to examine an individual generation of pRBCs exposed to this in vivo environment. To achieve this we used a modified version of our previous experimental approach (13). RBCs from mice infected with transgenic GFP-expressing *Pb*A parasites (*Pb*A-GFP^{pos}) were labeled with a fluorescent cell-tracking dye, CellTrace Far Red DDAO-SE (DDAO-SE), and transferred into recipient mice (Fig. 1*A*). Parasitized RBCs determined by flow cytometry as DDAO-SE^{pos}/GFP^{pos} indicated RBCs originating from the donor animals infected with a parasite from the donor mice [which we refer to as "generation zero" (Gen$_0$) of the donor cells] (Fig. 1*B*). Recipient mice either were naive or had been infected 5 d previously with non–GFP-expressing *Pb*A (*Pb*A-GFP^{neg}). The parasitemia of GFP^{neg} parasites in the acutely infected mice at the start of the experiment was 4.2% ± 0.2%. RBCs from donor mice composed 3.1% ± 0.1% and 3.6% ± 0.1% of the total RBCs in naive and acutely infected mice 1 h after transfusion, respectively. The transfer of GFP^{pos} parasites allows tracking of parasites from the donor animals in mice experiencing an ongoing *Pb*A-GFP^{neg} infection (Fig. 1 *A* and *B*). In a change from our previous approach in which a mixture of ring, trophozoite, and schizont stages had been transferred (13), the transfused donor pRBCs were semisynchronized such that most (~64%) parasites were in the ring stage at the time of transfer. This approach facilitated flow cytometric assessment and mathematical modeling of parasite maturation within RBCs, as well as measurements of PMF and removal of circulating pRBCs.

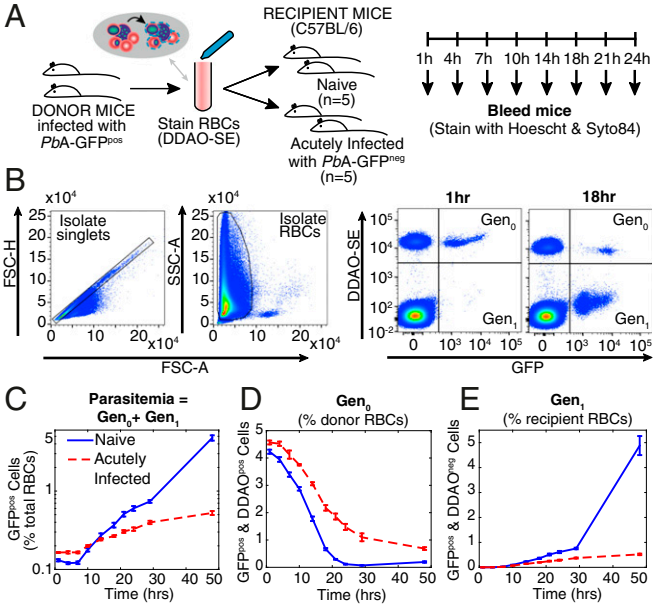

Fig. 1. Adoptive transfer protocol. (*A*) Donor mice infected with *Pb*A-GFP^{pos} had blood taken by cardiac puncture, and the red blood cells (RBCs) were labeled with DDAO-SE, washed, and transfused into groups of recipient mice. The recipient mice either were naive ($n = 5$) or had an ongoing acute infection with *Pb*A-GFP^{neg} ($n = 5$). Regular blood samples were taken from the recipient mice after transfusion, and the samples were stained for DNA and RNA before being analyzed by flow cytometry. (*B*) Representative flow cytometric data collected from one mouse in the naive mouse group, at 1 h and 18 h after transfusion. Forward scatter area and height (FSC-A and FSC-H) were used to isolate singlets, and side scatter area (SSC-A) and FSC-A were used to identify RBCs. The presence of the DDAO-SE stain indicated cells that originated from the donor mice, and GFP expression identified cells that were infected with parasites originating from the donor animals. This allowed identification of the first generation of pRBCs injected into recipient mice (called Gen$_0$) and those cells that had become infected with PbA-GFP^{pos} parasites posttransfusion (called Gen$_1$). We see Gen$_0$ parasites are lost over time, and there is a corresponding increase in the Gen$_1$ parasites. (*C*) The growth in (*Pb*A-GFP^{pos}, that is, Gen$_0$ + Gen$_1$) parasitemia over 48 h in recipient mice. Growth of parasitemia was lower in acutely infected mice compared with naive mice. (*D*) However, the difference in the growth in parasitemia did not appear to be accompanied by faster removal of Gen$_0$ parasites themselves. Rather, Gen$_0$ parasites persisted in circulation for longer in acutely infected mice than in naive mice. (*E*) The rate at which recipient RBCs (DDAO-SE^{neg}) become infected provides a direct measure of the rate of invasion of RBCs.

Consistent with previous findings (12–14), the growth of GFP^{pos} donor parasites in acutely infected mice (PMF = 2.0 ± 0.1) was less than half that observed for naive controls (4.6 ± 0.3) over 24 h ($P = 0.01$, Mann–Whitney test) (Fig. 1*C*). This reduction was previously attributed to increased removal of parasites from circulation (12). Therefore, we next sought to directly measure parasite removal from circulation by tracking Gen$_0$ pRBCs originating from the donor mice (i.e., DDAO-SE^{pos}/GFP^{pos}) in the bloodstream of naive and 5-d infected recipient mice.

In naive recipients, most Gen$_0$ donor pRBCs had disappeared from circulation by 24 h, probably due to maturation and RBC rupture according to the 24-h life cycle (Fig. 1*D*). In contrast, in 5-d infected recipients Gen$_0$ donor pRBC levels remained substantially higher than in naive controls (Fig. 1*D*; 32% ± 2% of initial concentration by 24 h after transfer compared with 2.7% ± 0.4% for naive controls; $P = 0.008$, Mann–Whitney test). It was particularly surprising that Gen$_0$ donor pRBCs appeared to be persisting beyond 24 h, because they were expected by this time to have ruptured and produced the next generation of parasites (20). This result was consistent across four repeat experiments in WT mice. This result was also consistent when the donor and recipient parasite lines were switched, confirming that this result was not the product of differences in the fitness of the GFP^{pos} transgenic parasite compared with the GFP^{neg} parasite (Fig. S1). Together, our analysis indicates that reduced growth of the circulating parasite population was associated, not with an increase in pRBC removal, but with an unexpected persistence of individual pRBCs in circulation.

Parasite Maturation Is Slowed Down During Infection. Given that the Gen$_0$ pRBC donor circulated longer than the usual 24-h life cycle of *Pb*A would permit, we next hypothesized that maturation of Gen$_0$ pRBCs was impaired during acute infection and tested this using an established flow cytometric approach (13, 21–23). In naive mice, ring-stage Gen$_0$ pRBCs (Fig. 2*A*) developed into more mature stages by 10 h, before mature forms disappeared from circulation likely due to a combination of RBC rupture and tissue sequestration (Fig. 2 *B* and *C*). However, in 5-d infected recipients, Gen$_0$ pRBCs were substantially impaired in their maturation, with ring-stage pRBCs persisting for longer than 10 h and the peak in mature-stage parasites occurring later (Fig. 2*C*). We next fitted a mathematical model of slower maturation (described in *Mathematical Model of Impaired Parasite Maturation*) to the data (Fig. 2*C*) on life-stage progression in these Gen$_0$ donor parasites. This modeling revealed that the maturation time in naive mice was not significantly different from 24 h ($P > 0.5$, comparing nested models with F test). Therefore, holding the maturation rate for parasites in naive mice to 24 h, we found that the progression of parasite life stages was ~40% slower in 5-d infected animals compared with naive animals ($P < 0.0001$, comparing nested models with F test), which increased the parasite life-cycle time from 24 h to 40 h.

A possible confounder that could lead to the apparent persistence of Gen$_0$ pRBCs would be the undesired reinvasion of the uninfected donor RBCs, which were transfused along with the Gen$_0$ pRBCs, and a preference for donor RBCs in acutely infected mice. Even after including this factor in the model, our estimate of slower maturation was altered only slightly from 40% to 35% slower in acutely infected mice, that is, a 37-h cycle time (Fig. 2*C*,

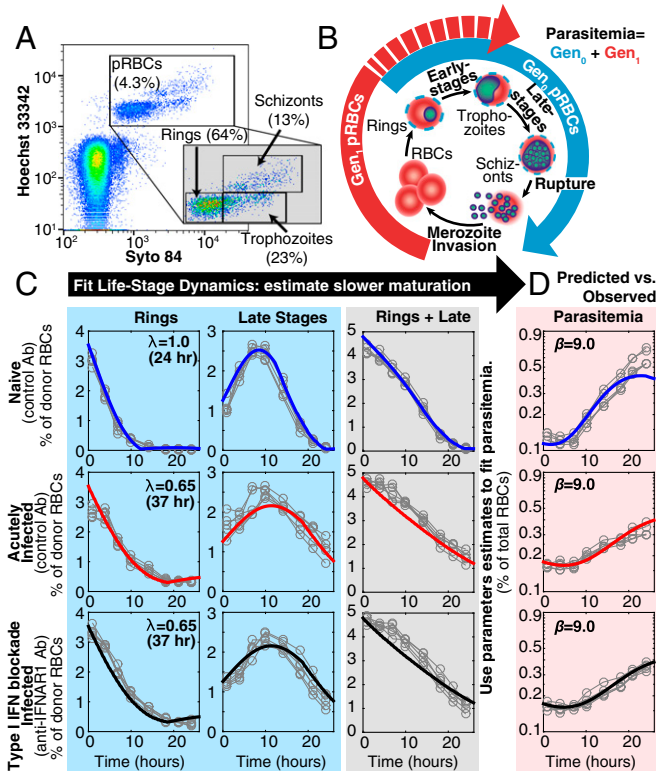

Fig. 2. Fitting the dynamics of Gen_0 and Gen_1 parasites. (*A*) DNA and RNA content was determined by flow cytometry and used to determine the proportion of Gen_0 parasites that were rings, trophozoites, and schizonts at each time point. (*B*) Illustration of how parasites progress through their asexual life cycle from young stages (rings) to late stages (trophozoites and schizonts), which then rupture and infect other RBCs. (*C*) The dynamics of Gen_0 parasites (GFP^{pos} and DDAO-SE^{pos}) in naive ($n = 5$) and acutely infected mice ($n = 5$), as well as mice with antibody-inhibited type-I IFN signaling (IFN-I^{neg}) ($n = 5$), were fitted using a mathematical model. The model (solid thick lines) provided a good fit of the dynamics of Gen_0 parasites (data: gray circles). All parameters were held to be equivalent between the three groups and estimated from fitting ($P_0 = 4.77\%$, $\mu = 0.32$ d, $\sigma = 0.26$ d, $c = 0.89$ d^{-1}), with the parasite maturation rate (λ), and, in the model reported here, the invasion ratio in donor RBCs was assumed to be nonzero and allowed to vary between groups (fitting estimates $\beta_D = 0.05, 0.44, 0.47$ for naive, acutely infected, and infected IFN-I^{neg} mice, respectively), and we estimate a significantly slower parasite maturation rate in acutely infected mice compared with naive mice ($P < 0.0001$, F test). In the model reported here we fixed the maturation time of parasites in naive mice equal to 24 h. The overall dynamics of Gen_0 parasites are shown in the gray column as the sum of rings and late stages. (*D*) Fitting the data on the parasitemia of GFP^{pos} parasites ($Gen_0 + Gen_1$) parameters, using the model and parameter estimates obtained from fitting the Gen_0 data in *C*. The only parameters estimated in fitting these data were the starting concentration of parasites from the donor mice as a percentage of total RBCs for each group of mice ($P_0 = 0.11, 0.18, 0.17$) and the invasion ratios in each group of mice, the latter not significantly different between groups ($P = 0.16$, F test).

Fig. S2, and *Invasion of Donor Cells*). The addition of parameters to allow for the possibility of different clearance rates of parasites between naive and acutely infected mice did not significantly improve the fits to the data ($P = 0.10$, F test). These observations suggest that *Pb*A maturation within RBCs can be altered by the host environment and therefore does not necessarily occur at a constant rate in vivo.

Slower Maturation of Parasites Accounts for the Majority of Reduced Parasite Growth. We next considered whether slowed parasite maturation could account for reduced parasite growth and lower PMF observed in 5-d infected mice (Fig. 1*C*). To do this we applied our mathematical model for Gen_0 pRBCs and the parameters obtained from fitting these data and attempted to predict parasite progression to the next generation (i.e., Gen_1, Fig. 2*B*). After fixing all of the parameters in our model to those estimated from fitting the data for Gen_0 (Fig. 2*C*), with the exception of a new parameter, the merozoite invasion ratio (β, average number of RBCs infected by a rupturing pRBC), and the initial parasitemia of donor pRBCs (P_0 in each group), we fitted this model simultaneously to the data for naive and acutely infected mice (Fig. 2*D*). From this fit, we estimated the parameter $\beta = 9.0$ (implying that each rupturing parasite produced 9.0 new infected cells). The remarkably good fit to the data when using the same invasion ratio for both naive and 5-d infected animals suggests that slow maturation, rather than other factors such as increased clearance of pRBCs or merozoites, explains the reduced growth rate of parasitemia observed in 5-d infected mice (the underlying mechanisms are discussed in *Understanding How Slower Maturation Mediates Control of Infection* and Fig. S3). When we extended the modeling to allow for different merozoite invasion ratios for naive and 5-d infected animals, looking for evidence of immune control in 5-d infected animals, we found that using different invasion ratios did not provide a significantly better fit ($P = 0.16$, F test), suggesting that slower maturation alone could completely account for the reduction in PMF in acutely infected mice.

Slow Maturation of *Py* Parasites. To confirm that our observations were not a *Pb*A-specific phenomenon, we repeated the adoptive

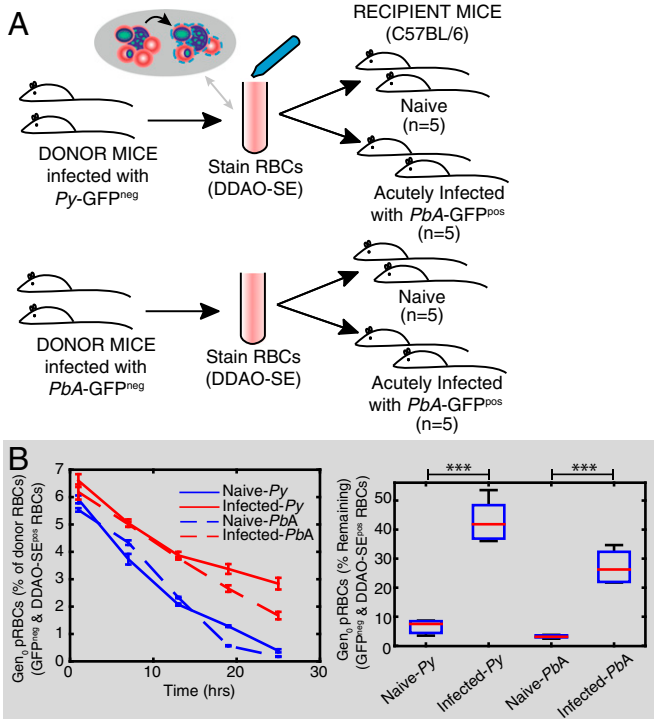

Fig. 3. Slower maturation of *Py* in acute infection. (*A*) Donor mice, infected with either *Py*-GFP^{neg} or *Pb*A-GFP^{neg} had blood taken by cardiac puncture, and the red blood cells (RBCs) were labeled with DDAO-SE, washed, and transfused into groups of recipient mice. The recipient mice either were naive or had an ongoing acute infection with *Pb*A-GFP^{pos}. Regular blood samples were taken from the recipient mice after transfusion, and the samples were stained for DNA and RNA before being analyzed by flow cytometry. (*B*) The percentage of donor *Py* or *Pb*A Gen_0 parasites remaining after transfusion compared with the initial concentration (measured as a percentage of total donor RBCs). Significantly more parasites remained in the circulation of acutely infected mice compared with naive mice after 25 h (***$P < 0.0005$, one-way ANOVA and contrast analysis).

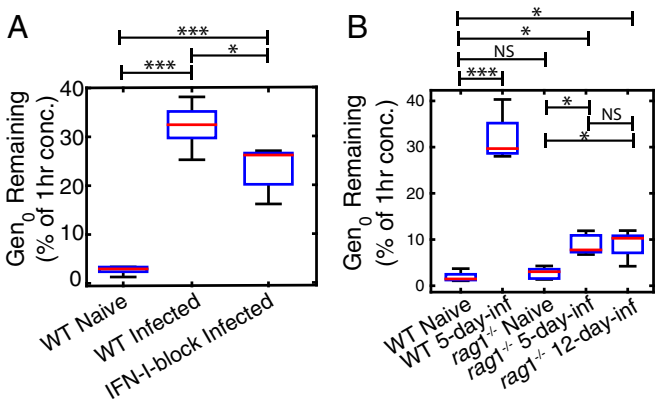

Fig. 4. Proportion of Gen_0 parasites remaining 24 h after transfusion. (*A*) We see a slight reduction in the proportion of parasites remaining at 24 h in acutely infected mice with blocked IFN-I signaling compared with acutely infected mice that received nonspecific control anitbody. (*B*) We see some increase in the proportion of Gen_0 parasites remaining at 24 h in acutely infected *rag1*$^{-/-}$ mice, but significantly less than the proportion of parasites remaining in acutely infected WT mice. NS, not significantly different; ***$P < 0.0005$, **$P < 0.005$, *$P < 0.05$.

transfer studies, using donor cells infected with *Py* into 5-d *Pb*A-GFP^{pos}–infected mice (Fig. 3*A*, Fig. S4, and P. yoelii *Infection*). We observed that like *Pb*A, *Py*-infected pRBCs persisted in circulation beyond their typical life-cycle times in acutely infected mice (Fig. 3*B*). Further, fitting our mathematical model revealed that *Py* parasites had a maturation time significantly shorter than 24 h (22 h, $P = 0.03$, *F* test). However, *Py* parasites matured 22% slower in acutely infected mice (29 h maturation time) compared with in naive mice ($P < 0.0001$, *F* test). These observations suggest that the maturation cycle of *Py,* like *Pb*A, can also be altered by the host environment.

Host Responses Contribute to Slower Parasite Maturation. Given that the reduced parasite maturation rate was observed only a few days into the infection, we next investigated a possible role for host inflammatory responses in mediating this phenomenon (14). To begin exploring this, we first blocked type-I IFN cytokine signaling via the receptor IFNAR1, because our previous data had suggested this innate immune signaling pathway could influence circulating pRBC numbers and life stages in vivo (24) (Fig. 2*C*). However, blockade of type-I IFN signaling did not significantly alter the extent to which parasite maturation was slowed in acute infection, compared with acutely infected, control-treated mice (comparing nested models with *F* test, $P = 0.50$; Fig. 2*C*), nor did it substantially affect the invasion ratio, β ($P = 0.16$, *F* test). Although it did marginally alter the persistence of circulating Gen_0 pRBCs (Fig. 4*A*). This was consistent across two repeat experiments. Taken together, our analysis suggested that signaling via a single cytokine receptor, IFNAR1, may influence the capacity of the host to modulate parasite maturation rate, but not substantially.

We next considered whether multiple host inflammatory responses might serve to impair parasite maturation. We used *rag1*$^{-/-}$ mice, which lack T and B cells and, most importantly, mount poor systemic inflammatory responses during infection, including weak production of TNF and IFNγ (*Cytokine Responses in rag1*$^{-/-}$ *and WT Mice* and Fig. S5) (14). The maturation rate in naive and *rag1*$^{-/-}$ mice was not significantly different from 1 (i.e., 24 h cycle time, $P = 0.13$, *F* test), nor was it significantly different from that in the naive WT mice ($P = 0.10$, *F* test). Further, compared with acutely infected WT mice, in which parasite maturation slowed by 31% (35-h cycle time) during acute infection (Fig. 5), Gen_0 pRBCs exhibited little impaired maturation in 5-d infected *rag1*$^{-/-}$ mice, slowing only by 10% (27-h cycle time) (Fig. 5); this was significantly faster than in the acutely infected mice ($P < 0.0001$, *F* test), but significantly slower than in the naive *rag1*$^{-/-}$ mice ($P = 0.01$, *F* test). This was a consistent trend across two repeat experiments. Even when donor parasites were injected into 12-d infected *rag1*$^{-/-}$ mice [where the recipient (GFP^{neg}) parasitemia was 13% ± 2% at the time of injection, compared with 6.9% ± 0.6% in 5-d infected WT mice and 2.6% ± 0.1% in 5-d infected rag1$^{-/-}$ mice], their maturation was still not dramatically slowed (no significant differences between 5-d and 12-d infected *rag1*$^{-/-}$ mice; $P > 0.5$, *F* test) (Fig. 5). Together, the maturation rate of parasites in *rag1*$^{-/-}$ mice, even in the presence of very high parasitemias, suggests that the phenomenon of slowed parasite maturation is dependent to a large degree on the host's response to infection.

Discussion

In this study we provide evidence of a host-mediated mechanism for controlling circulating blood-stage *Plasmodium* parasites

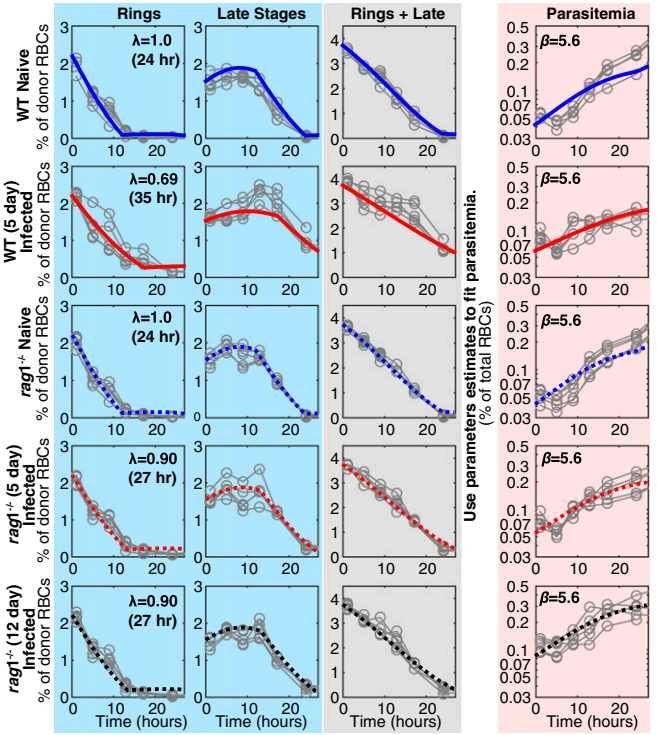

Fig. 5. Fitting the dynamics of infection in WT and *rag1*$^{-/-}$ mice. Gen_0 were sorted into ring stages and mature stages (blue panel), using flow cytometry. The dynamics of Gen_0 parasites were fitted using a mathematical model in which all parameters were the held to be equivalent between the five groups and estimated from fitting ($P_0 = 3.73\%$, $\mu = 0.30$ d, $\sigma = 0.50$ d, $c = 0.39$ d^{-1}), with the exception of the maturation rate, λ, and the invasion ratio in donor cells ($\beta_D = 0.073$, 0.22, 0.089, 0.14, 0.13, for WT naive, WT infected, *rag1*$^{-/-}$ naive, *rag1*$^{-/-}$ 5-d infected, and *rag1*$^{-/-}$ 12-d infected, respectively). We observed that the maturation rate in 5-d infected WT mice was significantly slower than the maturation rate in 5-d infected *rag1*$^{-/-}$ mice (*F* test, $P < 0.0005$). However, there was no significant difference in the maturation rates of parasites in 5-d and 12-d infected *rag1*$^{-/-}$ or between naive WT and naive *rag1*$^{-/-}$ mice ($P > 0.5$ and $P = 0.10$, respectively). The gray panel shows the overall dynamics of Gen_0 parasites (rings + late stages). Extending the model to consider rupture of mature parasites and invasion of RBCs (including the invasion ratio parameter, β), we used the parameter estimates from fitting the Gen_0 parasites (blue panel) to predict dynamics of the overall parasitemia (Gen_0 + Gen_1, red panel). Fitting this extended model to the parasitemia data (red panel), we estimated $\beta = 5.6$ (not significantly different between groups, all comparisons $P > 0.05$) and the starting concentration of parasites from donor mice as a percentage of total RBCs for each group ($P_0 = 0.042\%$, 0.059%, 0.042%, 0.054%, 0.083%, for WT naive, WT infected, *rag1*$^{-/-}$ naive, *rag1*$^{-/-}$ 5-d infected, and *rag1*$^{-/-}$ 12-d infected, respectively).

during acute infection, via the slowing of parasite maturation. This result is surprising, as *Plasmodium* infection is generally thought to be characterized by a regular life cycle with a periodicity expressed in multiples of 24 h that is often thought to synchronize with the host's diurnal rhythms (6, 25, 26). In *P. berghei*, for example, the parasite cycle time is thought to be of the order of 24 h in naive mice (20), consistent with our observations in naive mice. However, there are a number of precedents for altered *Plasmodium* life-cycle kinetics in vitro and in vivo. In vitro, for example, reduced availability of isoleucine has been shown to slow the maturation rate of *P. falciparum*, which has been estimated to have a 60% decrease in the rate of maturation through the parasite life cycle (27). This suggests that deprivation of nutrients could theoretically slow parasite development in vivo. However, the slower maturation we observe is not simply dependent on parasite density, as slow maturation is not observed in *rag*1$^{-/-}$ mice even at high parasitemia (Fig. 5). Thus, if the mechanism of impaired development is due to nutrient restriction, this restriction appears dependent on the presence of host responses that are altered in *rag*1$^{-/-}$ mice.

In vitro and in vivo studies have shown a significant variation in the maturation times for different strains of *P. falciparum* (1, 28), reinforcing the precedent for a nonfixed parasite life-cycle duration. In vivo the life cycle of the parasite is influenced by the diurnal rhythm of the host (25, 29). Parasite replication is significantly reduced when the parasite life cycle is mismatched with the diurnal rhythm of the host (25, 29). Further, in a number of animal models of infection it has been observed that the parasite adjusts to the rhythm of the host within a few life cycles (30, 31). This suggests that the parasite population on average will shorten or lengthen its life cycle in response to the host environment, to match the rhythm of the host. Interestingly, the presumably minor variations in host environment during the host diurnal rhythm must have major impacts on parasite replication, to synchronize host and parasite cycles over a few days (25, 29). It is perhaps not surprising that the large alterations in host environment during an acute inflammatory response to infection may also perturb the parasite life cycle. Therefore, an interesting line of inquiry would be to explore other parasite species, such as *Plasmodium chabaudi*, which typically produce quite synchronous infections that align with host diurnal rhythms and melatonin level (32). Because the maturation schedule in *P. chabaudi* is affected by diurnal factors in the host, the additional impact of host inflammation may lead to more complex patterns of parasite maturation.

Other studies suggest that drug treatment is also able to slow or halt (dormancy) the life cycle of *P. falciparum* parasites, which is thought to be a parasite stress response allowing parasites to survive treatment (33–37). Hence, it seems likely that slower maturation occurs as a parasite survival mechanism in response to environmental stress, perhaps as a result of the parasite directing resources to mitigate damage caused by some form of stress placed on the parasite, whether by drug or by the host environment. Thus, it is interesting to consider whether slower maturation could be considered a common adaptive strategy for parasite survival in a hostile environment.

The precise mechanism causing slower maturation in acutely infected hosts remains unclear. However, remembering that identical infected donor cells were transfused from the same donor mice into naive and acutely infected mice, host environmental factors must be able to act on already infected cells to influence the parasite development schedule. Further, it is clear from our study that this sensing of the environment by the parasite is rapid, because persistence of Gen_0 pRBCs was evident after the first time point (4 h, Fig. 1*D*). In addition, we have identified a key role for host factors in this process. Parasite maturation was not slowed in *rag*1$^{-/-}$ mice, which lack both T and B cells and have other abnormalities of lymphoid architecture. This does not imply that antigen-specific immunity is required for slow maturation, as T and B cells are known to also contribute to early innate immune responses through the production of cytokines (38–40). Indeed, when we compared early cytokine production in WT vs. *rag*1$^{-/-}$ mice, we found that *rag*1$^{-/-}$ mice show much reduced cytokine production from day 4 (Fig. S5) (14).

Previous studies have used a modeling approach to investigate the contribution of parasite clearance or reduced availability or susceptibility of uninfected red blood cells as mechanisms limiting parasite growth in acute infection (12, 13). However, these studies did not consider the possibility that parasite maturation rates could change in vivo. In this study, we specifically chose to transfer semisynchronous ring-stage Gen_0 pRBCs to facilitate an easier examination of parasite life stages. By using this approach we were able to observe the phenomenon of slowed parasite maturation. Our modeling approaches revealed that the observed slow parasite growth in 5-d infected mice can be completely explained once slow parasite maturation is considered. Despite the lack of evidence for faster clearance of pRBCs in this study, we cannot entirely exclude a role for increased splenic clearance during infection; but we have established that slow maturation has a major effect on overall parasite growth in these acute murine infections.

Our study clearly demonstrates that slow parasite maturation plays a major role in inhibiting parasite proliferation during acute blood-stage *Plasmodium* infection of mice. Moreover, the host response itself is required for slowing parasite maturation. Further work is needed to identify the exact molecular mediators of slower maturation. A major question is whether this process controls parasite growth in humans acutely infected with *P. falciparum*, where ethical and experimental limitations make this a challenging question to answer. Nevertheless, our in vivo observations provide unique insights into the dynamic nature of host–parasite interactions during acute blood-stage *Plasmodium* infection.

Materials and Methods

Experimental Mice and Ethics. Female C57BL/6J WT mice aged 6–12 wk were purchased from the Australian Resource Centre. Female C57BL/6J *rag1*$^{-/-}$ mice were bred at QIMR Berghofer Medical Research Institute and maintained under conventional conditions. All experimental groups in this study consisted of $n = 5$ mice. This study was carried out in strict accordance with guidelines from The National Health and Medical Research Council of Australia. All animal procedures and protocols were approved (A02-633M and A1503-601M) and monitored by the QIMR Berghofer Medical Research Institute Animal Ethics Committee.

Parasites, Infections, and in Vivo Treatments. *Pb*A and *Py* infections were initiated by defrosting frozen stabilates (200–300 μL) and injecting them into single WT C57BL/6J passage mice. Transgenic *Pb*A-GFP^{pos} strains were maintained as previously reported (41). Once parasitemia was patent on either day 3 or day 4 postinfection, passage mice were euthanized and infected blood was recovered by cardiac puncture. Acutely infected mice were generated by administering WT mice 10^5 pRBCs (*Pb*A-GFP^{neg} or *Pb*A-GFP^{pos}) i.v. via the lateral tail vein, using 26-gauge needles in a volume of 200 μL. *Pb*A- and *Py*-infected donor mice were generated by injection of defrosted stabilates as above. IFNAR1-blocking monoclonal antibody (clone MAR1-5A3; Leinco Technologies Inc.) or an isotype control antibody (Leinco Technologies Inc.) was administered in 0.1-mg doses in 200-μL vol, diluted with 0.9% Saline (Baxter), via i.p. injection (26-gauge needles) on days 0, 2, and 4 postinfection.

Adoptive Transfer of Donor RBCs. Donor mice were euthanized, and cardiac punctures performed to collect blood into lithium heparin tubes (1 mL MiniCollect; Greiner Bio-One). Heparinized blood was washed twice in Ca^{2+}/Mg^{2+}-free PBS (PBS-A) (Life Technologies) and stained in CellTrace Far Red DDAO-SE (Life Technologies) according to manufacturer's instructions. Briefly, 50 μg CellTrace was dissolved for 10 min in 25 μL dimethyl sulphoxide (DMSO). This was added to 5 mL of resuspended blood in PBS-A. Blood was stained in the dark, at room temperature with constant rolling for 15 min, and then washed twice in 10× vol PBS-A. Successful labeling of RBCs was confirmed by flow cytometry, using an LSRII Fortessa analyzer (BD Biosciences) and FlowJo software (Treestar). CellTrace-labeled blood was resuspended in 2-mL vol per donor mouse and injected in 200-μL vol via i.v. injection using a 26-gauge needle.

Flow Cytometric Analysis of Blood. Forward scatter (FSC) and side scatter (SSC) were used to distinguish RBCs from other cell types. Plotting FSC area (FSC-A) and FSC height (FSC-H) allowed the exclusion of doublets (events recorded by the flow cytometer that are the result of two cells being detected simultaneously). A flow cytometric method, adapted from various research groups (21–23), was used to simultaneously detect adoptively transferred (CellTrace-labeled) RBCs, to distinguish GFP^{pos} from GFP^{neg} parasites, and to ascertain parasite life-cycle stages. Briefly, a single drop of blood from a tail bleed was diluted and mixed in 200 μL RPMI medium containing 5 units/mL heparin sulfate. Diluted blood was simultaneously stained for 30 min in the dark at room temperature with the cell-permeant RNA/DNA stain, Syto84 (5 μM; Life Technologies) and with DNA stain, Hoechst 33342 (10 μg/mL; Sigma). Staining was quenched with 10 vol RPMI medium, and samples were immediately analyzed by flow cytometry, using an LSRII Fortessa analyzer (BD Biosciences) and FlowJo software (Treestar). Adoptively transferred donor RBCs were readily distinguished from endogenous RBCs by CellTrace labeling. Infected RBCs were detected as being Hoechst 33342^{+} and $Syto84^{+}$. Unless otherwise stated the concentration of infected donor RBCs (usually $DDAO\text{-}SE^{pos}$ and GFP^{pos} infected RBCs) is measured as a percentage of total donor RBCs (i.e., $DDAO\text{-}SE^{pos}$ RBCs).

Statistical Tests and Nonlinear Fitting. All errors reported in this paper are SEMs ($\pm\sigma/\sqrt{n}$). All comparisons of group means were performed using a one-way ANOVA followed by a post hoc contrast analysis [using the anova1.m and multcompare.m functions in MATLAB R2014b (8.4.0.150421)], unless otherwise stated. Nonlinear fitting of the models described in *Mathematical Model of Impaired Parasite Maturation* were performed using the constrained optimization function fmincon.m or the unconstrained optimization function fminsearch.m in MATLAB R2014b (8.4.0.150421). These functions minimize a user-specified function, which is the unweighted sum of squared residuals in this study (Figs. 2 and 5). When fitting the life-stage data for Gen_0 pRBCs (blue panels in Figs. 2 and 5), ring stages and late stages for all three groups were fitted simultaneously by minimizing the sum of all squared residuals (that is, the sum of squared differences between the model and all time points for all mice). When fitting the data for parasitemia (red panels in Figs. 2 and 5), the sum of squared residuals of the log-transformed data was minimized. Residuals between the model and all mice from each group were included in the sum of squares calculation. When testing whether the inclusion of additional parameters in a model was justified, an *F* test was used to compare the complete model to the restricted model (the full model but with some parameters fixed or set to zero). A parameter was determined to be significant if the hypothesis test showed that the restricted model was not supported by the data (i.e., $P < 0.05$).

ACKNOWLEDGMENTS. This work was supported by the Australian Research Council (Grant DP120100064) and the National Health and Medical Research Council (NH&MRC) (Grant 1082022 to M.P.D., D.C., and A.H.; Grant 1080001 to M.P.D.; and Grants 1028634 and 1028641 to A.H.). The Australian Federal Government provided Australian Postgraduate awards (to D.S.K. and K.R.J.). The University of Queensland (UQ) provided International Postgraduate Research scholarships (to I.S. and J.A.) and a UQ Advantage grant (to I.S.). M.S.F.S. and S.E.B. were supported by Australian NH&MRC Project Grants 613702 and 1028641.

1. Douglas AD, et al. (2013) Comparison of modeling methods to determine liver-to-blood inocula and parasite multiplication rates during controlled human malaria infection. *J Infect Dis* 208:340–345.
2. Roca-Feltrer A, et al. (2010) The age patterns of severe malaria syndromes in sub-Saharan Africa across a range of transmission intensities and seasonality settings. *Malar J* 9:282.
3. Doolan DL, Dobaño C, Baird JK (2009) Acquired immunity to malaria. *Clin Microbiol Rev* 22:13–36.
4. Pinkevych M, et al. (2014) Decreased growth rate of P. falciparum blood stage parasitemia with age in a holoendemic population. *J Infect Dis* 209:1136–1143.
5. Molineaux L, Träuble M, Collins WE, Jeffery GM, Dietz K (2002) Malaria therapy reinoculation data suggest individual variation of an innate immune response and independent acquisition of antiparasitic and antitoxic immunities. *Trans R Soc Trop Med Hyg* 96:205–209.
6. Kwiatkowski D (1989) Febrile temperatures can synchronize the growth of Plasmodium falciparum in vitro. *J Exp Med* 169:357–361.
7. Stevenson MM, Riley EM (2004) Innate immunity to malaria. *Nat Rev Immunol* 4:169–180.
8. Buffet PA, Safeukui I, Milon G, Mercereau-Puijalon O, David PH (2009) Retention of erythrocytes in the spleen: A double-edged process in human malaria. *Curr Opin Hematol* 16:157–164.
9. Evans KJ, Hansen DS, van Rooijen N, Buckingham LA, Schofield L (2006) Severe malarial anemia of low parasite burden in rodent models results from accelerated clearance of uninfected erythrocytes. *Blood* 107:1192–1199.
10. Jarra W, Brown KN (1989) Protective immunity to malaria: Studies with cloned lines of rodent malaria in CBA/Ca mice. IV. The specificity of mechanisms resulting in crisis and resolution of the primary acute phase parasitaemia of Plasmodium chabaudi chabaudi and P. yoelii yoelii. *Parasite Immunol* 11:1–13.
11. Smith LP, Hunter KW, Oldfield EC, Strickland GT (1982) Murine malaria: Blood clearance and organ sequestration of Plasmodium yoelii-infected erythrocytes. *Infect Immun* 38:162–167.
12. Metcalf CJE, et al. (2011) Partitioning regulatory mechanisms of within-host malaria dynamics using the effective propagation number. *Science* 333:984–988.
13. Khoury DS, et al. (2015) Reduced erythrocyte susceptibility and increased host clearance of young parasites slows *Plasmodium* growth in a murine model of severe malaria. *Sci Rep* 5:9412.
14. Khoury DS, et al. (2014) Effect of mature blood-stage Plasmodium parasite sequestration on pathogen biomass in mathematical and in vivo models of malaria. *Infect Immun* 82:212–220.
15. Buffet PA, et al. (2011) The pathogenesis of Plasmodium falciparum malaria in humans: Insights from splenic physiology. *Blood* 117:381–392.
16. Chotivanich K, et al. (2002) Central role of the spleen in malaria parasite clearance. *J Infect Dis* 185:1538–1541.
17. Del Portillo HA, et al. (2012) The role of the spleen in malaria. *Cell Microbiol* 14: 343–355.
18. Safeukui I, et al. (2008) Retention of *Plasmodium falciparum* ring-infected erythrocytes in the slow, open microcirculation of the human spleen. *Blood* 112:2520–2528.
19. Quinn TC, Wyler DJ (1979) Intravascular clearance of parasitized erythrocytes in rodent malaria. *J Clin Invest* 63:1187–1194.
20. Deharo E, Coquelin F, Chabaud AG, Landau I (1996) The erythrocytic schizogony of two synchronized strains of *plasmodium berghei*, NK65 and ANKA, in normocytes and reticulocytes. *Parasitol Res* 82:178–182.
21. Apte SH, Groves PL, Roddick JSP, P da Hora V, Doolan DL (2011) High-throughput multiparameter flow-cytometric analysis from micro-quantities of *plasmodium*-infected blood. *Int J Parasitol* 41:1285–1294.
22. Klonis N, et al. (2011) Artemisinin activity against *Plasmodium falciparum* requires hemoglobin uptake and digestion. *Proc Natl Acad Sci USA* 108:11405–11410.
23. Malleret B, et al. (2011) A rapid and robust tri-color flow cytometry assay for monitoring malaria parasite development. *Sci Rep* 1:118.
24. Haque A, et al. (2014) Type I IFN signaling in CD8- DCs impairs Th1-dependent malaria immunity. *J Clin Invest* 124:2483–2496.
25. O'Donnell AJ, Schneider P, McWatters HG, Reece SE (2011) Fitness costs of disrupting circadian rhythms in malaria parasites. *Proc Biol Sci* 278:2429–2436.
26. Mideo N, Reece SE, Smith AL, Metcalf CJE (2013) The Cinderella syndrome: Why do malaria-infected cells burst at midnight? *Trends Parasitol* 29:10–16.
27. Babbitt SE, et al. (2012) Plasmodium falciparum responds to amino acid starvation by entering into a hibernatory state. *Proc Natl Acad Sci USA* 109:E3278–E3287.
28. Reilly Ayala HB, Wacker MA, Siwo G, Ferdig MT (2010) Quantitative trait loci mapping reveals candidate pathways regulating cell cycle duration in Plasmodium falciparum. *BMC Genomics* 11:577.
29. O'Donnell AJ, Mideo N, Reece SE (2013) Disrupting rhythms in Plasmodium chabaudi: Costs accrue quickly and independently of how infections are initiated. *Malar J* 12:372.
30. Gautret P, Deharo E, Tahar R, Chabaud AG, Landau I (1995) The adjustment of the schizogonic cycle of Plasmodium chabaudi chabaudi in the blood to the circadian rhythm of the host. *Parasite* 2:69–74.
31. Taliaferro WH, Taliaferro LG (1934) Alteration in the time of sporulation of *Plasmodium brasilianum* in monkeys by reversal of light and dark. *Am J Hyg* 20:50–59.
32. Bagnaresi P, et al. (2009) Unlike the synchronous Plasmodium falciparum and P. chabaudi infection, the P. berghei and P. yoelii asynchronous infections are not affected by melatonin. *Int J Gen Med* 2:47–55.
33. Dogovski C, et al. (2015) Targeting the cell stress response of *Plasmodium falciparum* to overcome artemisinin resistance. *PLoS Biol* 13:e1002132.
34. Mok S, et al. (2015) Drug resistance. Population transcriptomics of human malaria parasites reveals the mechanism of artemisinin resistance. *Science* 347:431–435.
35. Cheng Q, Kyle DE, Gatton ML (2012) Artemisinin resistance in *Plasmodium falciparum*: A process linked to dormancy? *Int J Parasitol Drugs Drug Resist* 2:249–255.
36. Codd A, Teuscher F, Kyle DE, Cheng Q, Gatton ML (2011) Artemisinin-induced parasite dormancy: A plausible mechanism for treatment failure. *Malar J* 10:56.
37. Teuscher F, et al. (2010) Artemisinin-induced dormancy in *plasmodium falciparum*: Duration, recovery rates, and implications in treatment failure. *J Infect Dis* 202:1362–1368.
38. Bao Y, et al. (2014) Identification of IFN-γ-producing innate B cells. *Cell Res* 24:161–176.
39. Freeman BE, Hammarlund E, Raué H-P, Slifka MK (2012) Regulation of innate CD8+ T-cell activation mediated by cytokines. *Proc Natl Acad Sci USA* 109:9971–9976.
40. Kelly-Scumpia KM, et al. (2011) B cells enhance early innate immune responses during bacterial sepsis. *J Exp Med* 208:1673–1682.
41. Haque A, et al. (2011) Granzyme B expression by CD8+ T cells is required for the development of experimental cerebral malaria. *J Immunol* 186:6148–6156.